International Symposium on the Conservation of Monuments in the Mediterranean Basin

(2024)

Proceedings of the 11th MONUBASIN (2024)

Characterization and origin of ancient metallurgical slags from the ancient settlement of Archampolis, Euboea Island, Greece

Antonios Kontorozis, Michael Stamatakis, Eleftheria Dimou

doi: 10.12681/monubasin.8173

Characterization and origin of ancient metallurgical slags from the ancient settlement of Archampolis, Euboea Island, Greece

Antonios Kontorozis, *Department of Chemistry,* National and Kapodistrian University of Athens, Athens 15771, Greece
antonioskont@yahoo.com

Michael Stamatakis, *Department of Geology and Geoenvironment,* National and Kapodistrian University of Athens, Athens 15784, Greece
stamatakis@geol.uoa.gr

Eleftheria Dimou, *Department of Mineralogy and Petrography*, Hellenic Survey of Geology and Mineral Exploration, Spyrou Loui, Entrance G1, Acharnes 13672, Attica, Greece

Abstract. In the present study, metallurgical slags were investigated and characterized concerning their mineralogy, chemistry, and texture. The slag samples were collected close to the ancient village of Archampolis, located on southern Euboea Island, Greece. The aim of the study was to define the kind of archaeometallurgy, i.e., extraction of copper, silver, or iron, as well as to suggest possible sources of the ores which were used as raw materials burned in the kilns. Qualitative mineralogy and texture of the slags were performed using X-ray diffraction (XRD) and scanning electron microscopy (SEM-EDS). The determination of the major and trace elements of the samples was performed by X-ray fluorescence (XRF). By combining all analytical results, it was concluded that the metallurgy was applied for iron extraction, as the samples consisted of ferrous, glassy slags, while one sample was interpreted as a semi-melted host rock containing the original minerals. Geochemically, it turned out that certain slag pieces are enriched in Cu, As, Pb, and Tl, which indicates a possible origin of the initial ferric ore from the oxidization of the mixed sulfide ore. Such primary and oxidized polymetallic mineral deposits occur in the area of south Euboea Island, some of which have been exploited since the Antiquity. Another possible source could be Andros Island, being the closest area to Archampolis seawards, which hosts significant deposits of iron ores, most of them exploited for centuries.

Keywords: slags, ancient metallurgy, iron, wüstite, fayalite, Euboea

1 Introduction

The Aegean Region was one of the first to enter the Bronze Age in the Mediterranean. As such, there was an early development of metallurgy in the area, which included lead, silver, gold, copper and later iron. The metallurgy and craft specialization in the Aegean begins in the Late Neolithic-Early Bronze Age. The analysis of four models of boats made of lead that have been found in a burial of the Early Cycladic age (3400-2100 B.C.) on the island of Naxos suggested that the source of the ore was probably Siphnos Island (Gale and Stos-Gale, 1981). Lead is found in the Early Bronze Age record on several Cyclades islands, i.e., Antiparos, Despotikon, Kea, Syros, Amorgos, Ios, Milos, Kimolos, Anafi, Thera, and Naxos (Vaxevanopoulos et al., 2022). Lead metallurgy is also known in Early Bronze Age contexts in Cycladic settlements on the Raphina and Agios Kosmas coasts, Attica, on Crete, Lesbos, Lemnos and at Troy (Gale and Stos-Gale, 1981).

Several islands of the Aegean contain Pb-Ag-Zn (±Cu/As) mixed sulfide ores. Henceforth, since most of the lead ores in the Aegean and the Greek Mainland also contain Ag, the exploitation of lead was probably a key factor for the development of silver metallurgy as well, via a process known as cupellation. The earliest findings of metallurgy in Greece also include some rare gold objects from Macedonia dated in the latest stages of Late Neolithic at Sitagroi, Dikili Tash, Demetra, Aravissos, and

Proceedings of the 11th International Symposium on the Conservation of Monuments in the Mediterranean Basin, 17-19 of June 2024, Athens, Greece
https://doi.org/10.12681/monubasin.8173

the Early Bronze Age stages at Perivolaki (Photos, 1987). Literature data is indicative that northern Greece is most likely the richest gold-bearing region in Greece. However, evidence regarding the exploitation and production of gold deposits in the area during prehistory is poor (Vavelidis and Andreou, 2008).

The smelting of copper ores begins shortly after silver metallurgy, and copper objects, as well as slags, broken crucibles, and furnace linings, occur in the Late Neolithic age in Mainland Greece in a number of places, which include tin, arsenical and more rarely antimonial bronzes (Photos, 1987; Tylecote, 1992; Pelton et al., 2014; Nerantzis et al., 2016; Nerantzis et al., 2017). In Crete, the beginnings of metallurgy appear in Early Minoan I (2400-2200 B.C.), and the main center seems to be in the Mesara plain in the south. Most of the finds of this period are arsenical coppers, and dilute bronzes (3.14, 3.16% Sn) do not appear until the Middle Minoan I (2000 B.C.). These findings suggest that tin supply was heavily depended on trade routes and whenever there was a shortage of it, Sb and As local sources were used as an alternative solution (Tylecote, 1992).

The Iron Age in Greece began towards the end of the 11th century B.C. The use of iron is considered to have started earlier in South Greece than in Macedonia, though the dating remains uncertain (Photos, 1987). From the LBA (1600-1200 B.C.), there is ample evidence of iron metallurgy in various places of Greece in the form of rings, small plaques pendants, nails, rings, and knives but also metallurgical slags (Waldbaum, 1980; Photos, 1987; Backe-Forsberg et al., 2006). However, even though during the 1050-900 B.C., there are findings of an the abundance of iron artefacts, the replacement of bronze with iron is a slow process. Bronze alloys continue to be dominant in this period as well as in the next centuries, while it is used for spearheads and arrow tips (Photos, 1987). The aim of the present study is to analyze slag samples in order to define the kind of metals extracted in Archampolis and also to suggest possible sources of the raw materials which were burned in the kilns.

2 Geological Setting

The studied area is located in the southeastern part of Euboea Island, which comprises the Attic-Cycladic Massif (ACM) and is a member of the Intermediate Tectono-metamorphic Zone of the Hellenides orogen (Papanikolaou, 1984).

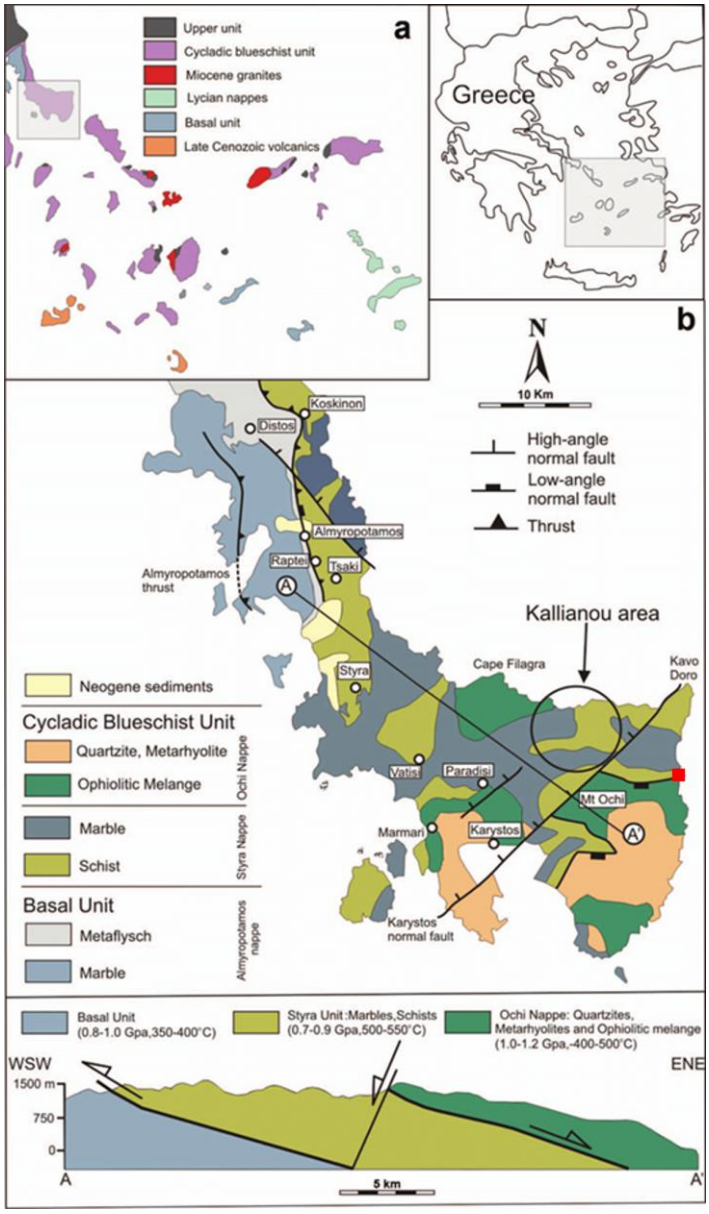

Fig.1: Simplified geological map of Southern Euboea with the Kallianou area marked in a circle and the Archampolis area with a red square (modified from Bindi et al., 2013)

The ACM was created during the Alpine orogeny and consisted of metamorphic rocks created in High Pressure / Low Temperature (HP/LT) conditions. The Karystos area consists of two litho-stratigraphic units: the "Styra" Nappe and the "Ochi" Nappe. The "Styra" Nappe is the local appearance of the Northern Cyclades Unit on the island of Euboea (Papanikolaou, 1978a; 1978b). It is comprised of a 2000m thick sequence of marbles with interlayers of schists and quartzites, metapelites along with metabasites and serpentinite lenses near the base of the nappe. The schists are mostly composed of muscovite, chlorite, quartz, and calcite, and rarely amphibole and epidote. The marbles are fine-grained to medium-grained and usually transition to cipolines. The schist in the upper horizons of the unit constitutes a metamorphic "wild flysch" with blocks of meta-ophiolites and other lithologies (Papanikolaou, 1978a; 1978b). The tectonically overlaying "Ochi" nappe is situated in the southernmost part of Euboea and has at least a 2500m thickness. The unit is mainly composed of metavolcanic, metabolites, meta hornfels, calcareous schists, quartzite interlayers, quartz-feldspar schists, and gneiss. Scarce lenses of mafic and ultramafic meta-igneous rocks are found in Ochi nappe, but mainly along the tectonic contact with the underlying Styra nappe. The contact of the two nappes is an ENE-directed shear

zone rather than a discrete fault surface (Xypolias et al., 2010; Ring et al., 2007). This unit has been associated by Papanikolaou with the Makrotantalon Unit in northern Andros Island, where there have been found marble horizons with Permian fossils (Papanikolaou, 1976; 1978a; 1978b). The unit underwent blueschist-facies metamorphism at 18kbars and 550^{o}C. Afterward, a retrograde greenschist-facies metamorphism followed at 4-9kbars and 450-550^{o}C during the exhumation of the unit. The beginning of the metamorphism was dated in the Upper Cretaceous around 105-75 Ma, which was followed by the blueschist-facies metamorphism in Upper Eocene (ca 45-35 Ma) and finally, the retrograde greenschists-facies metamorphism around 25-20Ma (Bröcker & Franz, 1998; 2006; Zeffren et al., 2005). However, to this day, the unit's position in the tectonostratigraphic terranes is a matter of debate. Some researchers propose that the Ochi unit represents the ophiolitic mélange of the Cycladic Blueschist Unit (CBU) (Papanikolaou, 1978a; 1978b; 1987; Ring et al., 2007; Shaked et al., 2000), while others consider it as part of the Pelagonian Zone (Blake et al., 1981; Bonneau, 1982; Dürr, 1986; Huet et al., 2015) or the Upper Unit of the ACM metamorphic core complex (Katzir et al., 2000).

3 Mineralization

The southern Euboea is a part of the Attic-Cycladic-Pelagonian ore belt, which includes base- and precious-metal skarn, intrusion-related, and epithermal mineralization deposits. Most specifically, the Karystos area consists of the metamorphic formations of Northern Cyclades nappe and the overlying Makrotantalon – Ochi nappe, as mentioned earlier. The two types of mineralization in southern Euboea are mixed sulfide and manganese ores.

3.1 Mixed sulfides mineralization

The mixed sulfides mineralization located in the Kallianou area (Fig.1) has been exploited mainly for its golden-silver-rich ore since ancient times (Voudouris et al., 2011). The indicated size of the Kallianou deposit is estimated to be 500,000 tonnes at an average grade of 2-2.4% Pb, 0.7% Zn, 0.5-0.8% Cu, 35-60 g/t Ag and 5 g/t Au (Alexouli-Livaditi, 1978; Katsikatsos, 1978). According to Alexouli-Livaditi (1978), Theofilopoulos and Vakondios (1982), Perlikos (1988) and Vavelidis and Michailidis (1990), the mineralization in the Kallianou area covers an area of about 50 Km^2, north of Karystos. The host rock of the sulfides is the metapelites (mica schists) and the marbles of the Styra nappe. The mineralization occurs either within monomictic tectonic breccias in the hanging–wall marble unit along the contact with the schists or as meter-thick quartz veins that crosscut the foliation of the footwall schists (Voudouris et al., 2011). The quartz veins that are enriched in mixed sulfides ore contain up to 52 g/t Au and 242 g/t Ag (Alexouli-Livaditi, 1978). These veins have a general NW direction with a 30-70^{o} NE dip (Theofilopoulos and Vakondios, 1982). Breccia in the marble unit consists of angular fragments of the host rock cemented mainly by quartz, chlorite, albite, and carbonate minerals. Galleries, shafts, and dumps of rock waste are found in the area, suggesting intense mining activity since antiquity.

Metallic mineral facies of the ore include pyrite, arsenopyrite, löllingite, argentite, electrum, native silver, gold, various Ag-Cu tellurides, etc. (Alexouli-Livaditi, 1978; Vavelidis and Michailidis, 1990; Voudouris and Spry, 2008). Pyrite, galena, and chalcopyrite are the most common metallic minerals. Chalcopyrite postdates pyrite andreplaces pyrite along with galena. Sphalerite participates as a minor phase and is closely related to chalcopyrite (Alexouli-Livaditi, 1978). The latter one is often found as inclusions in the former (Varelidis and Michailidis, 1990). It is notable that Ag does not replace Pb in the crystal lattice of galena, but it is present as an inclusion of Ag-bearing sulfotellurids. The main gangue minerals of the ore-rich veins include quartz and calcite, while the wall rock alteration consists of chlorite, muscovite, albite, and calcite (Voudouris et al., 2011). The veins postdate the ductile deformation associated with the HP/LT metamorphism of the Miocene. As for the mechanism responsible for the formation of the deposit, two theories have been proposed. The first one proposes that the hydrothermal fluids have originated from a granitoid intrusion during the cooldown (Vavelidis and

Michailidis, 1990; Alexouli-Livaditi, 1978). The second one argues for the introduction of metals during retrograde greenschists-facies metamorphism (Theofilopoulos and Vakondios, 1982; Perlikos 1989).

According to Sakharova et al. (1981), Au hydrothermal deposits are formed at temperatures ranging between 50° and 250°C (Vavelidis and Michailidis, 1990). According to Voudouris et al. (2011), the maximum temperature for the formation of the Kallianou quartz veins was considered to be about 300°C. This temperature estimate is based on the study of Nüchter and Stöckhert (2007), who proposed that microfabrics in the discordant quartz veins in the metamorphic rocks of the broad Kallianou area indicate deformation around 300°C, at a depth just below the brittle-ductile transition. Similar temperatures (290-310°C) were estimated by chlorite geothermometry for the formation of quartz veins hosted within retrograde metamorphic rocks of the CBU unit in central Euboea Island (Voudouris et al., 2008). Furthermore, the fahlore and polybasite assemblages' composition suggests that they were formed at temperatures below 200°C in the Kallianou area.

3.2 Manganese mineralization

The manganese occurrences in the broad Karystos area are located near the village of Stoupeoi and on the beach of St. Demetrius. These occurrences are overlying (tectonically) the mixed sulfides mineralization. Furthermore, while the mixed sulfides ore is confined in an area close to the hypothetical igneous intrusion, the manganese ores are widespread even at distances of several kilometers in the northern direction (Perlikos, 1989).

The manganese occurrences can be classified into two groups:

- The first group is hosted into quartzites (Andronopoulos, 1962). The ore is scattered in three separate quartzite horizons, which are located in the middle and the upper sections of the quartz-mica schists. These horizons stretch from an area north of the village of Aetos to the villages of Frygana and Pano Kampos. They are discontinuous and can be described as a disseminated mineralization of manganese lenses, which have undergone small-scale exploitation in the past (Dimou et al., 1997).
- The second group of manganese ores is found in quartzitic-micaceous schists and occurs in scattered areas north of village Aetos and up to the ravine of St. Demetrius and the Stoupeoi village. These occurrences are stratified with ore bands alternating with gangue.

The occurrences of the two groups are probably related stratigraphically, as suggested by neighboring occurrences of the two ore groups north of Aetos village in the Panagia and Tsiftiliki locations (Perlikos, 1989). The primary minerals of the ore are braunite and hausmanite, while secondary minerals such as pyrolusite, holandite, and piemontite were described (Andronopoulos, 1962; Perlikos, 1988).

Other types of mineralization. According to Latsoudis and Triantaphyllis (1997), who carried out a detailed geological mapping in the area of southern Euboea, mineralizations of iron-manganese and iron-copper also exist.

4 Iron metallurgy in antiquity

The Iron Age started in the second millennium BC. The forging of man-made iron was sporadic at the beginning, but gradually, the production increased to meet the demands for weapons around 1200-1100 BC. The greater ductility of iron swords in comparison with tin and led bronzes gave them a significant advantage, as they could withstand more blows without breaking (Tylecote, 1992). As a result, the need for improved weaponry created the knowledge of ironworking. The technology of ironworking is divided into two sections: smelting and hot forging. The melting point of pure iron is at 1538°C, and this temperature was unachievable by early smiths up until the 19th century AD, with the invention of the

blast furnace. Thus, all early wrought iron was produced in a solid state by chemical reduction of iron ore to solid iron at about 1200ºC, using charcoal as a reducing agent (Tylecote, 1992).

According to Tylecote (1987), in antiquity, two types of furnaces were used for iron smelting: the bowl furnace and the shaft furnace. In the bowl furnace, the iron ore, along with coke, is placed in a hole in the ground, which is coated by loam. Then, fresh air was pumped through tuyere in the bowl furnace. The air reacted with the hot coke to form CO. Thus, the iron ore was provided with a continuous supply of CO, which was progressively reducing the ore to metallic iron (Vaxevanopoulos, 2017).

The shaft furnace was developed as the technology of ironworking was improving and became dominant until the discovery of the blast furnace. It consisted of a vertical stone structure, usually above a pit. The structure was cylindrical and had a coating of loam in its interior. Coke mixed with iron ore was supplied from the top of the furnace structure (Papadopoulos and Nerantzis, 2012). In the upper layers of the shaft furnace, the iron minerals (e.g. $FeCO_3$) are broken down at temperatures around 500ºC. In the lower layers, reducing conditions were developed at 750ºC, where the produced CO participated in the reduction of iron oxides (Vaxevanopoulos, 2017), according to the following equation:

$$FeO + CO \rightarrow Fe + CO_2$$

The reduced iron was removed as lumps called “bloom”, which was a mixture of solid iron, slag and pieces of unburnt charcoal. In order to extract the iron from the slags, the lumps were broken down and the iron fragments were separated with hot hammering at a temperature of 1200ºC approximately (Zianni, 2012).

4.1 Metallurgical slags

The undesired impurities of the ore, alongside fluxes, remnants of fuel, and ceramics from the walls of the furnace or the tuyere and some iron remnants, were merged and created slags. Since most of the slag components had a lower melting point than iron, the slags were in a liquid or semi-liquid state in the furnace. As a result, they were concentrated in the bottom of the pit and exited the shaft furnace through a hole into the surrounding area. In antiquity, the slags were left in situ once the metal was collected because their transportation would be costly and pointless. Therefore, the existence of slags is an indicator of metallurgical activity in the area. Depending on the quantity of the ore used, slags could form heaps or be scattered lumps in the broader area of the furnace. Their existence is important because they often are the sole evidence of the metallurgical activities in ancient Greece (Saiti, 2017).

4.2 Archampolis

During antiquity, the Ravine of Archampolis was a settlement related to extensive ironworking (Panagopoulou, 1994; Dimou et al., 1997). Dating of the findings uncovered by excavations suggest that the area was inhabited during the 5th to 1st century BC, but there is evidence of a Geometric period settlement that is yet to be uncovered or was already destroyed by the 5th century BC. The settlement was under the influence of the city of Karystos during the classic period, as revealed by two bronze coins of Karystos and three of the Euboean League, of which Karystos was an active member.

5 Materials and methods

5.1 Materials

The slag samples studied (Fig.2) were collected by the broad area of Archampolis in the southern part of Euboea Island. The slags are found on the northern side of Archampolis Gulf at the outlet of the gorge and occupy an area of about 200 m^2. The slope displays a great inclination (35-45º) and is affected by strong winds, a basic element for the process of smelting. The slags have a dark brown, black, or bluish color and are found approximately 800 m away from the archaeological excavations area (Dimou et al.,

1997). No stratigraphic sequence in the slag deposition area was observed, so sampling was conducted at random points. For the present paper, 9 slag samples were selected for analysis, representing different textural features, named ARPL1 to ARPL9 (Fig.2).

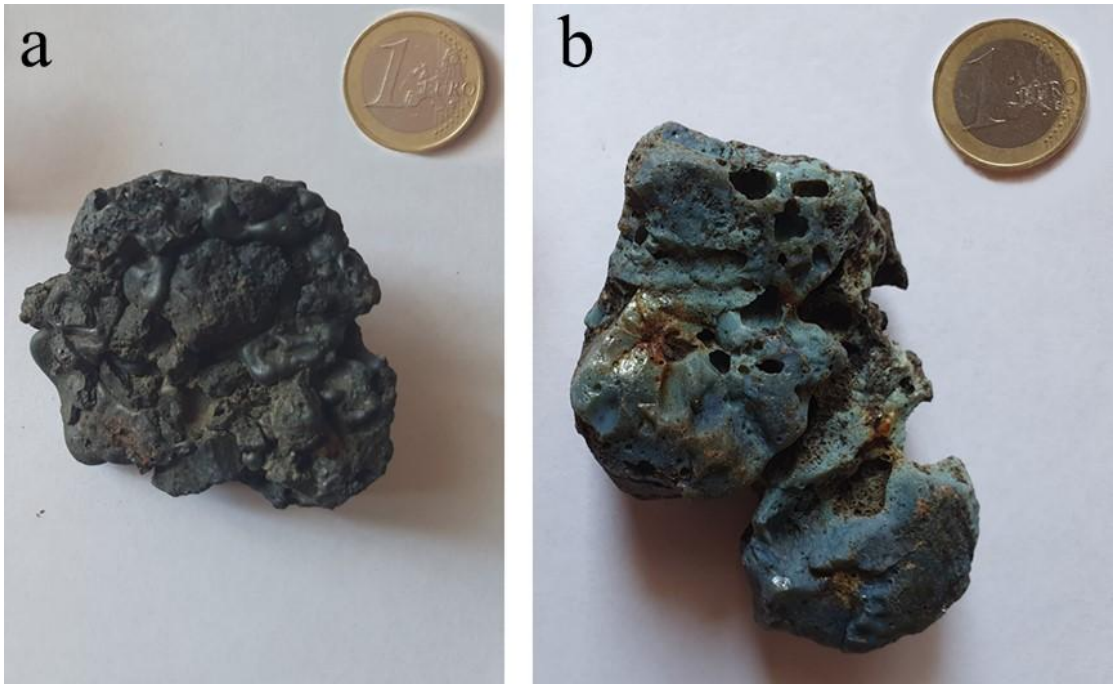

Fig 2: Representative samples of Archampolis slags. (a) Ferrous slag (ARPL-1) and (b) glassy slag (ARPL-8)

5.2 Analytical methods

The methods used for the determination of mineralogical phases were X-ray diffraction (PXRD) and electron Microprobe Analysis (SEM-EDS), while the elemental composition of the samples was determined by X-ray Fluorescence (XRF) technique. The XRD analysis was conducted by TITAN S.A. using the D8 ADVANCE Diffractometer model of Bruker Corp. The evaluation of the results was conducted with EVA v5.2 software, a part of the DiffacPlus package of Bruker Corp, in a Windows environment. The XRF analysis was conducted in TITAN S.A. R&D labs located in Eleusis, using the Bruker 58 TIGER spectrometer. The SEM-EDS analysis was conducted in the lab of the Mineralogy and Petrology Department of the Faculty of Geology and Geoenvironment, NKUA, using a JEOL JSM-5600 scanning electron microscope equipped with an EDS micro-probe type Oxford Link ISIS 300. Operating conditions were 20kV and 0.5 nA with a beam diameter of 3μm (CuKa X-ray line).

6 Results

6.1 XRD patterns

All samples analyzed by the XRD method. The mineralogical analysis revealed that the main component of the slags is wüstite (FeO), followed by fayalite, quartz, and bustamite ($CaMnSi_2O_6$). All the other minerals occur in smaller amounts or only in certain samples (Table 1). In addition to crystalline mineral phases, the presence of amorphous silica glass was deduced in all samples from the hump between 20-

26º on the XRD patterns. The most noticeable humps were detected in samples ARPL6 and ARPL9, indicating higher concentrations of glassy matrix.

Table 1: XRD mineral analysis of the Archampolis slags*

SAMPLES	WUSTITE	FAYALITE	BUSTAMITE	QUARTZ	ALBITE	ANORTHITE	CALCITE	TEPHROITE	MAGHEMITE	GOETHITE	DOLOMITE	HEMATITE	MAGNETITE	GARNET	PYROXENE	LIME	MELILITE	MICA/ILLITE	CHALCOPYRITE	HORNBLENDE	CORUNDUM
ARPL1	MJ	MD		TR			TR	MJ						TR		TR			TR		
ARPL2	TR		MJ	MD			TR														
ARPL3	MJ	MD		MD	TR		TR									TR					
ARPL4				MD	MJ	MJ	MD						TR					TR		TR	
ARPL5	MJ	MD		MD	TR		MD						TR			TR					
ARPL6			MJ	MJ	TR		MD										TR				
ARPL7	MJ			MD					MJ	MD			MD		TR		TR				TR
ARPL8			MJ	MD	TR		MJ				MJ	TR									
ARPL9			MJ	MJ	MD		MD					TR		TR	MD		TR				

*: Explanatory notes: MJ = major component, MD = medium component, TR= minor/trace component

6.2 XRF analysis

XRF analysis was used to determine the elemental composition of samples ARPL1 –ARPL9. Major elements are presented as oxides and trace elements as parts per million (ppm) in Tables 2a and 2b. It is noted that in the XRF analysis, the total iron concentration is referred to as Fe_2O_{3t}. However, this does not mean that the samples contain exclusively Fe^{+3}. In fact, as the XRD patterns show, all samples contain mostly Fe^{+2} with traces of Fe^{+3}.

Table 2a: XRF analysis for major elements oxides, Archampolis slags

%	ARPL-1	ARPL-2	ARPL-3	ARPL-4	ARPL-5	ARPL-6	ARPL-7	ARPL-8	ARPL-9
SiO_2	9,8	46,28	12,47	50,92	5,73	47,28	50,77	48,84	46,2
Al_2O_3	2,26	6,94	2,77	14,96	1,37	7,76	8,04	8,01	7,51
Fe_2O_{3t}	77,53	6,06	73,55	12,12	88,82	2,98	2,93	2,89	2,64
CaO	4,42	11,19	4,06	6,46	1,66	11,75	15,65	15,61	11,01
MgO	0,62	2,58	0,49	4,75	0,17	3,97	2,4	2,45	2,96
SO_3	0,19	0,31	0,21	0,16	0,22	0,34	0,32	0,32	0,41
Na_2O	0,19	0,48	0,27	5,11	–	0,58	0,46	0,47	0,66
K_2O	0,32	2,72	0,28	0,55	0,11	2,96	3,1	3,09	2,68
TiO_2	0,14	0,31	0,2	2,11	0,08	0,34	0,35	0,35	0,33
MnO	5,97	22,51	4,68	0,56	2,57	22,21	16,07	16,08	26,01
P_2O_5	0,58	0,05	0,54	0,37	0,31	0,02	0,04	0,04	0,03
LOI				1,28				0,74	
SUM	101,83	99,43	101,52	99,35	101,04	100,19	100,13	100,91	100,44

Table 2b: XRF analysis for trace elements, Archampolis slags

Elements (ppm)	ARPL-1	ARPL-2	ARPL-3	ARPL-4	ARPL-5	ARPL-6	ARPL-7	ARPL-8	ARPL-9
V	71	56,9	207	266	28,9	21,1	10,2	19,8	21
Cr	208	347	54,2	51,5	114	280	61,9	245	318
Co	0	0	16,2	30,3	0	0	0	0	0
Ni	21,3	10,3	117	8,5	37,2	9	123	13,7	18
Cu	259	21,5	25,6	105	360	43	2117	27,8	12,1
Zn	32,1	7,9	9,1	163	9,8	16	33,8	4,3	5,9
Ga	14,7	14,1	0,7	22,9	9,5	11,1	6,6	9,4	14,6
Ge	0,7	0,7	9,9	0,7	0,7	0,7	0,7	0,7	0,7
As	8,2	1,2	11,9	3,1	7,5	10,5	1036	3	0,7
Br	0	0,1	0	0,2	0	0,1	13,1	0,1	0,1
Se	11,6	8	0	2,9	10,9	8,5	5,2	9	7,4
Rb	0	37,5	80,6	8,1	2,5	40,1	30,3	52	39,1
Sr	86,2	595	9,7	141	19,5	560	35,9	506	569
Y	10,5	60,4	22,1	28,2	3,5	82,6	0	54,1	73,7
Zr	21,1	59,6	2,5	123	15,9	65,4	19,8	65	65,3
Nb	3,1	3,4	2	14,3	2,5	3,3	0,6	2,1	2,3
Mo	4,3	1,6	1,4	1,8	3,8	0,9	12,8	0,5	0,3
Ag	0,6	2	0,1	0,8	1	6,4	1,2	2,4	8,3
Cd	0,3	0,5	2	0,3	0,5	0	1,1	0	0,1
Sn	1,8	0	7,2	1,5	1,4	0	10,1	0,3	0
Sb	8,8	0,3	2,7	0,3	10,4	0,7	52,6	1,2	1,5
I	2,8	0	3,6	0,6	2,5	0	2,5	0,8	0
Te	0,4	0	1,3	0,6	0,1	0	2,2	0,8	0,9
Cs	3,4	3,7	645	3,8	5,1	3,4	3,2	3,1	2,8
Ba	867	1578	16,2	99	335	5552	179	1717	7250
La	11,5	46,2	7,9	26	8,4	53,9	7,5	44,7	39,1
Sm	8	12,1	22,9	7,6	5,9	13,2	7,7	11	9,6
Ce	20,3	72,2	24	55,6	14,6	81,4	16,7	68,4	68,4
Nd	31,2	70,6	120	32,2	10,8	129	12,7	67,5	136
Yb	4,9	0	3,7	0	39,1	0,6	0	0	26,8
Hf	5,5	11	56,4	0	0	9,9	0	11,9	12,9
W	65,7	30,8	0,7	22,7	76,6	34,3	61,2	33,1	39,2
TI	2028	437	47,6	20,8	925	192	193	89	198
Pb	47,1	0	0	224	42,1	0,8	158	2,1	1,2
Bi	0	0	0	0	0	0	0	0	0
Th	0	3,8	9,9	0	0	5,3	0	1,2	1

7 Discussion

The Cyclades area, of which southern Euboea is a part, belongs geologically to the Attic-Cycladic Massif and was affected by two orogenic episodes: one in the Late Jurassic-Early Cretaceous and one in Late

Eocene-Oligocene. During the Middle-Late Miocene, the Anatolian microplate, by moving westwards, started to push the Aegean area southwards. The result of these movements was to speed up the subduction velocity, creating a back-arc extension regime in the ACM. Under these conditions, the exhumation of the metamorphic core complex and igneous intrusions were favored. One such intrusion is hypothesized to have created the Fe-Pb-Cu-Zn mixed sulfides mineralization in southern Euboea and Andros islands, the center of which is located in the Kallianou area. The discovery of slag heaps near the ancient settlements of Archampolis and in northern Andros (Ipsili, Palaiopolis)suggests that the abundance of ferrous deposits drove a rapid development of ironworking in the Aegean Sea.

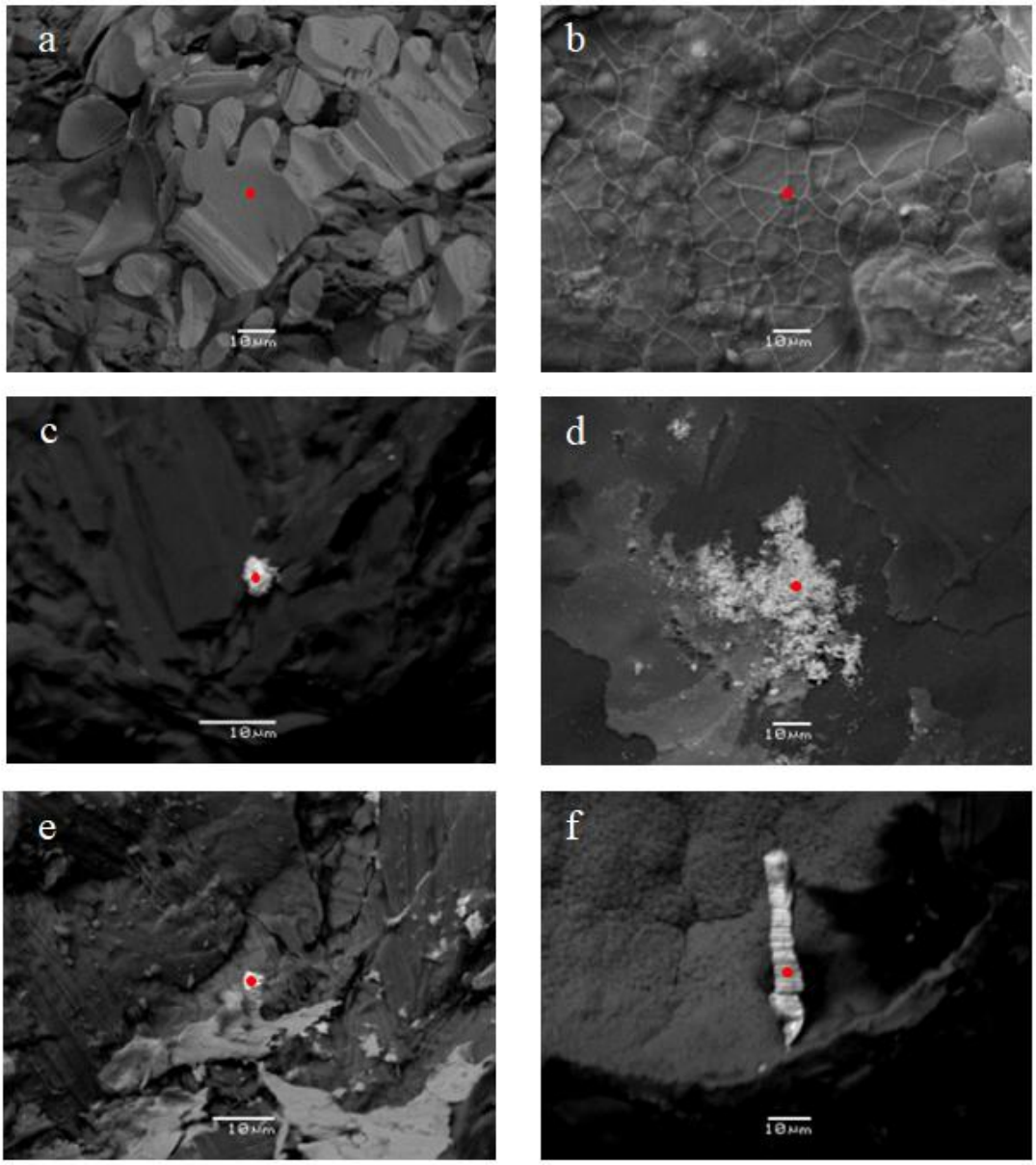

Fig 3: Granules of (a) wüstite, (b) Mn-rich fayalite, (c, d) prills of galena and cerussite, (e) cuprite-cassiterite and (f) cassiterite, marked by the red do*t*

Before examining the origin of the initial material used to extract the iron, the melting condition in the furnace must be understood. However, the various melting points of the artificial minerals and the glassy phase created in the furnace complicate this task, especially if flux agents were used, such as manganese oxides. As was mentioned earlier, charcoal was used to reduce the ore, which produced CO. The reduction of iron, however, was not usually achieved in one stage but rather in several ones. As a

result, magnetite was formed below 300ºC and wüstite between 300-1000ºC as intermediate products (Tylecote 1992). Furthermore, in temperatures ranging between 1000 and 1200ºC, wüstite reacts with SiO_2 to form fayalite. Sheikh et al. (2010) studied ferrous slags from the 4th century BC in India and concluded that the furnace in which they were produced was working at 1250-1300ºC, given the fact that fayalite has a melting point of 1205ºC and the wüstite-fayalite eutectic point is at 1177ºC.

The presence of the series of calcareous olivines of monticellite-kirschstenite, where monticellite ($CaMgSiO_4$) is the manganese member and kirschstenite is the ferrous end-member of the series, is significant to determine the smelting temperatures. Mukhopadhyay and Lindsley (1983), while studying mixtures of fayalite-kirschstenite, discovered that the Ca-olivines were formed at 1165-1170ºC, while fayalite formed at 1100º C, under CO-CO_2 atmosphere. Correspondingly, Sharp and Mittwed (2011), by examining fayalite-kirschstenite-rich slags, found that the intermediate glassy phase was formed at temperatures of 1100-1200º C, which is also shown in the FeO-SiO_2-Al_2O_3 ternary diagram. A similar pattern was observed while analyzing the ferrous slags of Andros Island. When plotted in the ternary diagram SiO_2 – FeO (+MnO + CaO) – Al_2O_3, the slags occupy an area between pure $FeSiO_4$ and optimum 1 point, which signifies the maximum concentration of SiO_2 in the melt for fayalite to form (Stamatakis, 2018).

In both samples from Archampolis and Andros the MnO could not be reduced in the furnace, so instead reacts with SiO_2 to form Mn-Fe-Ca-silicates, which make up the glassy matrix. As a result, in Andros slags, crystallization starts with metallic iron, followed successively by wüstite, mineral phases which are formed from the reaction of FeO with SiO_2 (fayalite, bustamite, tephroite, kirschstenite), and finally glass of melilite composition (Stamatakis, 2018). On the contrary, in Archampolis samples, the glass is composed almost exclusively of bustamite, fayalite, and tephroite, depending on the concentration of manganese in the sample. Kirschstenite was not detected, but in one sample, the magnesium end-member of the series, monticellite ($CaMgSiO_4$), was found. The fact that Fe does not form Ca-silicate minerals on its own, but prefers to substitute the Mn in bustamite is probably caused by the high concentration in MnO of the samples, which was maybe used as a flux agent. Also notable is the absence of the melilite group minerals, with the exception of samples ARPL6 and ARPL9. In ARPL6, åkermanite ($Ca_2MgSi_2O_7$) was detected, while in ARPL9, the composition of the melilite was $Ca_{5,95}Na_{2,05}[Si_2O_7]_2$, according to the XRD analysis. This phenomenon is probably due to the low concentrations of Na_2O and Al_2O_3 in the samples, which are usually trapped in the albite crystal lattice in the rock formations of the study area and, henceforth, not available in the melt.

According to the XRF analysis, the samples can be classified into two categories, regarding their chemical composition:

1. Fe-rich samples, with $Fe_2O_{3t} > 70\%$
2. Silica-rich samples with $SiO_2 > 45\%$

7.1 Fe-rich samples

Fe-rich samples constitute residual iron (II) oxide, which was not fully reduced to metallic iron (Fig 2a). This group includes the samples ARPL1, ARPL3 and ARPL5. They are made up mostly of wüstite (FeO), which is found in spheroid to botryoid granules sunk in a fayalitic matrix (Fig.3a, b). SEM-EDS analysis revealed that fayalite is of the manganese variety, detected mostly in ARPL1 and ARPL3 samples. Moreover, in sample ARPL1, where the maximum concentration of MnO (5.97%) for this group was detected, the glassy matrix is dominated by tephroite, the manganese end-member of the olivine group. The lowest concentration of MnO (2.57%) is found in the ARPL5 sample (Table 2a), while the ARPL3 contains 4.68% MnO, which results in the formation of the intermediate member of fayalite-tephroite series, knebelite $(Fe, Mn)_2SiO_4$. These results are in accordance with the findings of Dimou et al. (1997), who measured 4-8% content of MnO in fayalites of the Archampolis slags.

The maximum concentration of Mn in wüstite granules was detected in the ARPL1 sample (3.9% MnO). According to the XRD patterns (Table 1) and the SEM-EDS analysis, the Fe-rich slag samples also contain the following trace minerals:

- ARPL1: Spessartine, a-quartz, lime (CaO), calcite, rutile
- ARPL3: a-quartz, calcite, lime (CaO), albite
- ARPL5: a-quartz, calcite, anhydrite, ilmenite, lime (CaO), albite, magnetite, siderite, brownmillerite [$Ca_2(Al, Fe)_2O_5$]

Concerning the mechanism of ancient shaft furnaces described beforehand, the presence of iron minerals such as magnetite and siderite can be attributed to a partial reduction of iron ore. Oxides like rutile (TiO_2) and ilmenite ($FeTiO_3$) could be primary or authigenic, formed due to the reducing conditions inside the furnace. The presence of calcite and lime can possibly be sourced from the marbles, pipelines, and calcareous schists hosting the mineralization. When heated to 1200^{o}C, the calcite was transformed to lime. A part of the lime could be trapped inside the wüstite clumps, while the rest reacted with the CO_2 of the atmosphere and reverted to calcite. Another possible source of these phases could be chunks of refractory coating (loam) trapped within the slags. The presence of chalcopyrite in the ARPL1 sample is an indication that the source of the ore was probably the mixed sulfides mineralization located in the area and, more specifically, the oxidized parts of it. Furthermore, in samples ARPL3 and ARPL5, two baryte crystals, a gangue mineral accompanying hydrothermal mineralizations, were observed in SEM. Their presence further supports the aforementioned theory about the source of the iron ore. Anhydrite crystals are also present in the samples. Minerals like spessartine and brownmillerite could have been formed during the cooling of the glassy matrix. The quartz could either have formed also by the crystallization of glass or preexist as part of the source material since it is known that the mixed sulfides in southern Euboea are found inside quartz veins.

7.2 Silica-rich (glassy) samples

In this group belong the samples ARPL2, ARPL4, ARPL6, ARPL7, ARPL8 (Fig. 2b) and ARPL9. Among them, ARPL4 and ARPL7 stand out due to the drastic divergence of their mineral composition in comparison with the rest of the group. ARPL4 is composed mainly of minerals of the plagioclase group (albite, anorthite) and secondarily by a-quartz, calcite, magnetite, illite, hornblende, and muscovite (Table 1). The sample is likely a semi-melted host rock (schist) that contained the ore. As Dimou et al. (1997) have pointed out, muscovite and hornblende are characteristic minerals of the metamorphic rocks of the basement rocks in the studied area. The XRD pattern of ARPL7 shows mainly iron phases, though the XRF analysis (Table 2a) showed concentrations of only 2.9% Fe_2O_3t, 16.07% MnO, and 50.77% SiO_2. Sample analysis showed the presence of mineral facies such as wüstite, maghemite (g-Fe_2O_3), goethite, a-quartz, grossular, halloysite, monticellite, åkermanite, spinel, corundum, magnesite, jadeite, lepidocrocite and a substantial amount of glassy matrix (given the hump and kurtosis of the XRD pattern). It may represent a transition zone between the wüstite-fayalite phase at the bottom of the furnace and the manganese glassy phase, which, according to Bachmann (1980), is formed in the upper layers of the furnace when the ore contains a substantial percentage of manganese. The rest of this group samples are glassy microporous slags, which have macroscopically a bluish hue. As observed by Dimou et al. (1997), the glass has undergone partial devitrification, though the extent of the phenomenon is not uniform in all samples. The maximum concentration of glassy matrix appears to be in samples ARPL6 and ARPL9, followed by ARPL8 and ARPL2. The concentration of MnO ranges between 26% (ARPL9) and 16% (ARPL8). According to Dimou et al. (1997), the microliths formed during the recrystallization are of bustamite composition ($CaMnSi_2O_6$), which is confirmed in this paper. Apart from bustamite, according to XRD patterns (Table 1), the glassy slags contain the following minerals:

- ARPL2: a-quartz, wüstite, calcite
- ARPL6: a-quarts, calcite, åkermanite, langbeinite $K_2Mg_2(SO_4)_3$, albite
- ARPL8: dolomite, calcite, a-quartz, christobalite, hematite, albite, siderite
- ARPL9: a-quartz, calcite, albite, melilite, diopside, hematite, grossular

Minerals such as quartz, cristobalite, langbeinite, grossular and siderite were formed by recrystallization of glass, while the samples also contain small quantities of iron ore that were not completely reduced (wüstite, hematite). As in ferrous slags, the presence of calcite is attributed to coating

chunks that were stripped off from the furnace's wall or alternatively to the host rock, while the albite probably remains as a relic mineral of the host rock of the mineralization. Finally, notable is the presence of many members of the melilite mineral group (melilite, åkermanite) and the pyroxene group (diopside). According to Bachmann (1982), melilite is formed when the ratio of MeO (metal oxides) to SiO_2 reaches 1.5:1 in the furnace, while pyroxenes when the ratio drops to 1:1. In conclusion, it is deduced that the sample ARPL9 is the most depleted in metal oxides, which is confirmed by XRD analysis, for all metals except for Mn.

7.3 Other metals in the slags

By SEM-EDS microprobe analysis, galena and cerussite granules (Fig.3c, d) were detected in samples ARPL4 and ARPL6 and Cu-As (Fig.3e) granules in ARPL7. Moreover, as it is shown in Table 2b, unusually elevated concentrations of thallium were observed in samples ARPL1 (2028 ppm) and ARPL5 (925 ppm), even though no thallium minerals were detected, as it probably entered in the lattice of neocrystallized Fe-rich minerals. Thallium is known to be present in high concentrations at hydrothermal environments below 200^{o}C, in relation to sulfides (Sobott, 1995) and especially pyrite, as a substitution of Fe in the crystal lattice (Lopez-Arce et al., 2017). These findings are in accordance with the theory proposed by Voudouris et al. (2011), who hypothesized that the mixed sulfides deposition in the Kallianou area took place at 300-200^{o}C. All evidence suggests that the primary iron mineralization was constituted by mixed sulfides while being a part of distant occurrences of the hydrothermal Kallianou system. Afterward, the ore was oxidized, resulting in the leaching of the more labile elements and the enrichment of iron in the form of Fe-oxyhydroxides. (Voudouris et al., 2011; Tombros et al., 2021). Possible sources of the raw primary ore could be the region of the southern Euboea (Kallianou and surroundings), and/or the neighboring Cyclades islands. Similar iron deposits derived from the alteration of mixed sulfides have been found in Andros, at the sites Paleopolis and Aghios Petros, where the iron ore contains residual pyrite, chalcopyrite, and a gold grain of 50 μm (Perlikos, 1988; Vasilatos, 1990; Strati, 2019). Also, high concentrations of Cu were detected in three samples (259 ppm in ARPL1, 360 ppm in ARPL5, and 2117 ppm in ARPL7), as well as 1036 ppm As in ARPL7. Furthermore, no high concentrations of Cr or Co were found in any sample (maximum 347 and 30 ppm, respectively).

To conclude this paper's findings, we must report that during the SEM-EDS analysis, a tin grain was found in ARPL5 and a Cu-Sn grain in the ARPL8 sample (Fig.3f). Given the fact that none of the samples showed Sn concentration above 10 ppm, it is rather improbable that the tin grains were part of the primary mineralization. Maybe the source of these grains was the various tools used to load the furnace with the ore-charcoal mix. In that case, this would be an indication of dating these slags in the Early Iron Age, where iron was still a luxury item used for jewelry and weapons. This indirect dating would be close to the oldest dating Keller (1984, 1985) proposed as the beginning of the settlement in the 7th century BC.

8 Conclusions

By combining all analytical results, it was concluded that metallurgy was applied for iron extraction. The original feeding material was most likely an oxidized polymetallic ore. Geochemically, it turned out that certain slag samples are enriched in Cu, As, Pb, and Tl. Thallium is known to be present in high concentrations at hydrothermal environments below 200^{o}C, in relation to sulfides and especially pyrite, as a substitution of Fe in the crystal lattice. These findings are in accordance with the theory proposed by Voudouris et al. (2011), who estimate that the mixed sulfides deposition in the Kallianou area took place at 300-200^{o}C. All these observations are indicative of a possible origin of the initial ferric ore from the oxidization of the mixed sulfide ore, which is located in the area of south Euboea Island. However, the neighboring island of Andros could also be an additional source of iron ores for the Archampolis metallurgical works.

9. Acknowledgments

Thanks are expressed to Ms. Katerina Nikolaou-Hartiati for providing the slag samples, Dr. Maria Panagopoulou for the fruitful discussions, Mr. Vasilis Skounakis, NKUA, for the SEM analysis and to Ms. Stella Tetsika, TITAN SA, for the XRF analysis.

10 References

1. Alexouli-Livaditi A., "The mixed sulfides ore of the Kallianou area, South Euboea Island", PhD Dissertation, National Technical University of Athens, p.125, (1978)
2. Andronopoulos V., "Geological composition of the south Euboea Island: geology, petrology, metallogeny", PhD Dissertation, National and Kapodistrian University, Athens, (1962)
3. Backe-Forsberg, Y., Gradin, L., Harthner-Holdar, E., Risberg, Ch. & Bassiakos, Y., "Ancient iron sources in southern Peloponnesus, Greece", 2nd International Conference for the Ancient Greek Technology, Athens, (2006)
4. Bachmann H.G., "Scientific studies in Early Mining and Extractive Metallurgy", London, British Museum, (1980)
5. Bachmann H.G., "The Identification of Slags from Archaeological Sites", Institute of Archaeology, University of London, Occasional Papers 6, (1982)
6. Bindi, L., Voudouris, P. & Spry, P.G., "Structural role of tellurium in the minerals of the pearceite-polybasite group", Mineralogical Magazine, 77, p. 419- 428, (2013)
7. Blake, M. C. J., Bonneau, M., Geyssant, J., Kienast, J. R., Lepvrier, C., Maluski, H. & Papanikolaou D., "A geological reconnaissance of the Cycladic blueschist belt, Greece", Geological Society of America Bulletin, 92, 247–254, (1981)
8. Bonneau, M., "Evolution géodynamique de l'arc égéen depuis le Jurassique Supérieur jusqu' au Miocène" (in French), Bulletin de la Société Géologique de France,7, 229– 242, (1982)
9. Bröcker, M., Franz, L., "Rb–Sr isotope studies on Tinos Island (Cyclades, Greece): additional time constraints for metamorphism, extent of infiltration-controlled overprinting and deformational activity", Geological Magazine 135, 369–382, (1998)
10. Bröcker, M., Franz, L., "Dating metamorphism and tectonic juxtaposition on Andros Island (Cyclades, Greece): results of a Rb–Sr study", Geological Magazine 143, 609–620, (2006)
11. Dimou, E., Economou, G., Markoylis, M., Pantelias, E., and Perdikatsis, V., "Contribution to the study of the ancient slags of Archambolis, Karystos area, Euboea Island, Greece", 2nd Southern European Conference on Archaeometry, Delphi, PACT, 45 (II), 6, (1997)
12. Dürr S., "Das Attisch-kykladische Kristallin", (in german) In: Jacobshagen, V. (ed.) Geologie von Grienchenland Gebruder Borntraeger, Berlin, 116–148, (1986)
13. Gale, N. H. and Stos-Gale, Z. "Lead and Silver in the Ancient Aegean" Scientific American 244, no. 6, pp. 176-193, (1981)
14. Huet B., Labrousse L., Monié P., Malvoisin B., & Jolivet L., "Coupled phengite ^{40}Ar–^{39}Ar geochronology and thermobarometry: P-T-t evolution of Andros Island (Cyclades, Greece)", Geological Magazine, 152(4), 711-727, (2015)
15. Katsikatsos G., "The mineral deposits in the area of Euboea County", IGME internal report (unpublished), p.27, (1978)
16. Katzir Y., Avigad D., Matthews A., Garfunkel Z. & Evans B., "Origin, HP/LT metamorphism and cooling of ophiolitic mélanges in southern Evia (NW Cyclades), Greece", Journal of Metamorphic Geology, 18, 699–718, (2000)
17. Keller D., "Archampolis: An Early Iron Age settlement and sanctuary in Southern Euboea", AJA 88, p. 249, (1984)
18. Keller D., "Archaeological survey in Southern Euboea; Greece: A reconstruction of human activity from Neolithic Times through the Byzantine period", Ph. D. Diss., Indiana University, (1985)
19. Latsoudis Ch. and Triantaphyllis M., "The geological map of Greece, 1: 50.000, sheet Karystos-Platanistos", IGME, Greece, (1997)
20. Lopez-Arce P., Garcia-Guinea J., Garrido F., "Chemistry and phase evolution during roasting of toxic thallium-bearing pyrite", Chemosphere, Vol. 181, pp. 447-460, (2017)
21. Mukhopadhyay D. K., Lindsley D. H., "Phase relations in the join kirschsteinite ($CaFeSiO_4$)-fayalite (Fe_2SiO_4)", American Mineralogist, Vol. 68, pp. 1089–1094, (1983)
22. Nerantzis N., Bassiakos Y., and Papadopoulos S., "Copper metallurgy of the Early Bronze Age in Thassos, north Aegean", Journal of Archaeological Science: Reports, Vol. 7, p. 574-580, (2016).

23. Nerantzis, N., Sanidas, G., Jagou, B., Kozelj, T., & Panoussi, K., "An Archaic metallurgical workshop in Thasos (Greece): the case of Charitopoulos plot", STAR: Science & Technology of Archaeological Research, Vol. 3(2), p. 148–160, (2017)

24. Nüchter, J.A., Stöckhert, B., "Vein quartz microfabrics indicating progressive evolution of fractures into cavities during postseismic creep in the middle crust", J. Struct. Geol., vol. 29, pp. 1445–1462, (2007)

25. Panagopoulou M., "Archampoli: Archaeological Research", (in Greek), pp.10-12, Athens, (1994)

26. Papadopoulos S., Nerantzis N., "The ironwork production in the broad region of Kavala during the historical era", In: "Kavala and the Balkans. Kavala and Thrace", (in Greek), Editor: Roudometoff B.N., Proceedings of the 3rd conference of Balkans historical studies, Vol. A', Kavala, (2012)

27. Papanikolaou D., "The age of crystallic schists in Andros Island", Acad. Of Athens Proceed., 51, pp.292-301 (in Greek), (1976)

28. Papanikolaou D., "Geologic Studies in Andros Island", Ph.D. Dissertation, NKUA, p.231 (in Greek), (1978a)

29. Papanikolaou D., "Contribution to the Geology of Aegean Sea. The island of Andros", Ann. Géol. Pays Hellén., 29/2, pp. 477-553, (1978b)

30. Papanikolaou D., "The three metamorphic belts of the Hellenides: a review and a kinematic interpretation", Spec. Publ. Geol. Soc. London, 17, pp. 551-561, (1984)

31. Pelton, A., Stamatakis, M. G., Kelepertzis, E., Panagou, T., "The Origin and Archaeometallurgy of a Mixed Sulphide Ore for Copper Production on the Island of Kea, Aegean Sea, Greece", Archaeometry, Vol. 57, Issue 2, pp. 318-343, (2014)

32. Perlikos P., "Primary metallogeny research in Southern Euboea and Andros Islands", (unpublished), IGME, pp. 75-99, Athens, (1988)

33. Perlikos P., "A new view of the geology and the ores of south Euboea Island" Bulletin of the Geological Society of Greece, 23, p. 327-344, (1989)

34. Photos, E., "Early Extractive Iron Metallurgy in N. Greece: a unified approach to regional archaeometallurgy", PhD Dissertation, University of London, (1987)

35. Ring, U., Glodny, J., Will, T. & Thomson, S., "An Oligocene extrusion wedge of blueschist-facies nappes on Evia, Aegean Sea, Greece: implications for the early exhumation of high-pressure rocks", Journal of the Geological Society, London, 164, 637–652, (2007)

36. Saiti N., "Characterization and origins of ancient metallurgical slags from the ancient theatre of Karthea, Kea Island", (in Greek), BSc, NKUA, Athens, (2017)

37. Sakharova, M. S., Batrakova, Y. A., and Ryakhovskaya, S. K., "The effects of pH on the deposition of gold and silver from aqueous solutions", Geochem. Intl., 18, p. 28-34, (1981)

38. Shaked, Y., Avigad, D. & Garfunkel, Z., "Alpine high-pressure metamorphism of the Almyropotamos window (southern Evia, Greece)", Geological Magazine, 137, 367– 380, (2000).

39. Sheikh M.R., Acharya B.S. and R.K. Gartia, "Characterization of iron slag of Kakching, Manipur by X-ray and optical spectroscopy", Indian J. Pure Applied Phys., Vol. 48, pp. 632-634, (2010)

40. Sobott R.J.G., "Minerals and calculated low-temperature phase equilibrium in the pseudoternary system Tl_2S–As_2S_3–Sb_2S_3", Miner. Petrol., Vol. 53, pp. 277-284, (1995)

41. Stamatakis M., "The ancient scoriae of the island of Andros. Geochemical and mineralogical determination and archaeometallurgical observations", In: "Paleopolis, Andros, thirty years of excavation research", L. Palaiokrassa-Kopitsa Editor, Kaeirios Library publication, Andros, p. 208-210, (2018)

42. Strati M., "Ore deposits of iron and manganese of Andros Island. Characterization and restoration suggestions of the mining district", BSc thesis, National and Kapodistrian University of Athens, pp. 210, (2019)

43. Theofilopoulos, D. & Vakondios. I., "Geological and mineralogic studies in the Kallianou area, NE Euboea Island", (in Greek), Mineral Wealth,19, p. 27-50, (1982)

44. Tombros, S., Kokkalas, S., St. Seymour, K., Voudouris, P., Williams-Jones, A., Zhai, D., Liu, J., Fitros, M., "The Kallianos Au-Ag-Te mineralization, Evia Island, Greece: a detachment-related distal hydrothermal deposit of the Attico-Cycladic Metallogenetic Massif", Mineralium Deposita, Vol. 56, pp.665-684, (2021)

45. Tylecote R.F., "The early history of metallurgy in Europe", Longman, London, pp.185-220 (1987)

46. Tylecote R.F., "A History of Metallurgy", 2nd Edition, Antony Rowe Ltd, London, pp. 47-60 (1992)

47. Vasilatos Ch., "Mineralogical and petrographic research on igneous formations and ores of Andros Island", (in Greek), unpublished Ph.D. Dissertation, National and Kapodistrian University, Athens, (1990)

48. Vavelidis M. & Michailidis K., "Cold composition in the Fe-Pb-Cu-(Ag-Zn) hydrothermal quartz veins of Kallianou area, Southern Euboea (Greece)", Bulletin Geological Society Greece, 22, p. 87-96, (1990)

49. Vavelidis, M. & Andreou, S., "Gold and gold working in Late Bronze Age Northern Greece", Die Naturwissenschaften. Vol. 95. pp. 361-6, (2008).

50. Vaxevanopoulos M., "Recording and Study of Ancient Mining Activity on Mount Pangaeon, E. Macedonia, Greece", Unpublished Doctoral dissertation (in Greek), Aristotle University of Thessaloniki, Thessaloniki, Greece (2017)
51. Vaxevanopoulos M., Blichert-Toft J., Davis G., Albarède F., "New findings of ancient Greek silver sources", Journal of Archaeological Science, Vol. 137, p. 105474, (2022)
52. Voudouris P., Spry P.G., "A new occurrence of cervelleite-like phases and Te- polybasite from gold-bearing veins in metamorphic rocks of the Cycladic Blueschist Unit, Greece", 33rd International Geological Congress, MRD-09 Au-Ag telluride-selenide deposits, CD-ROM, Abstract, (2008)
53. Voudouris P.C., Spry P.G., Sakellaris G.A., Mavrogonatos C., "A cervelleite- like mineral and other Ag-Cu-Te-S minerals [Ag_2CuTeS and $(Ag,Cu)_2TeS$] in gold- bearing veins in metamorphic rocks of the Cycladic Blueschist Unit, Kallianou, Evia Island, Greece", Miner Petrol., 101, 169–183, (2011)
54. Waldbaum J., "The first archaeological appearance of iron and the Transition to the Iron Age", in 'The Coming of the Age of Iron', T. A. Werthime and J. D. Muhly, (eds.), Yale University Press, pp. 69-98, (1980)
55. Xypolias P., Dimitris S., Chatzaras V., Kokkalas S., Koukouvelas I., "Vorticity of flow in ductile thrust zones: Examples from the Attico-Cycladic Massif (Internal Hellenides, Greece)", Geological Society Special Publication, 335, pp. 687-714, (2010)
56. Zeffren, S., Avigad, D., Heimann, A., Gvirtzman, Z., "Age resetting of hangingwall rocks above a Tertiary low-angle detachment, Tinos Island", Aegean Sea, Tectonophysics 400, 1–25, (2005)
57. Zianni A.-M., "The processing of copper and iron and the iron artefacts of the Late Bronze Age and Early Iron Age in Southern Greece", Ph.D. Dissertation, National and Kapodistrian University, Athens, (2012)